AD NUMBER
AD336950
CLASSIFICATION CHANGES
TO: unclassified
FROM: confidential
LIMITATION CHANGES
TO: Approved for public release, distribution unlimited
FROM: Distribution authorized to U.S. Gov't. agencies and their contractors; Administrative/Operational Use; JAN 1963. Other requests shall be referred to Defense Advanced Research Projects Agency, Washington, DC.
AUTHORITY
darpa ltr 11 jan 1974; darpa ltr 11 jan 1974

CONFIDENTIAL

CONFIDENTIAL

RESEARCH PAPER P-4

RATE-ENHANCED BURNING OF A PROPELLANT OBEYING A PYROLYSIS LAW (U)

F. A. Williams

JANUARY 1963

INSTITUTE FOR DEFENSE ANALYSES
RESEARCH AND ENGINEERING SUPPORT DIVISION

Contract SD-50

CONFIDENTIAL

The Institute for Defense Analyses produces three kinds of publication for distribution, entitled Report, Study, and Research Paper.

A Report embodies the results of a major research project undertaken by IDA and is intended to be an authoritative contribution on its subject.

A Study is a less formal document and less comprehensive in scope than a Report. It may be the result of a smaller and more narrowly defined research project or it may be a supporting technical paper prepared in connection with a major project.

A Research Paper represents the work of one or more named authors but is subject to review comparable to that for publication in a professional journal.

CONFIDENTIAL

RESEARCH PAPER P-4

RATE-ENHANCED BURNING OF A PROPELLANT OBEYING A PYROLYSIS LAW (U)

F. A. Williams

JANUARY 1963

INSTITUTE FOR DEFENSE ANALYSES
RESEARCH AND ENGINEERING SUPPORT DIVISION

IDA/HQ 63-1062
Copy 23 of 50 copies

CONFIDENTIAL

RATE-ENHANCED BURNING OF A PROPELLANT OBEYING A PYROLYSIS LAW

by F. A. Williams

I. INTRODUCTION

It has been found empirically[1] that by inserting wires in a solid propellant grain, the burning rate of the propellant can be increased by a factor of 5 or 10. The shape of the burning propellant surface becomes a series of cones, with their vertices centered on the wires. Heat conduction from the hot gas, along the highly thermally conductive wire, into the propellant, serves to maintain the conical shape of the surface. The phenomenon provides one useful method for obtaining increased propellant burning rates in a motor that is subjected to various geometrical restrictions.

The purpose of the present paper is to develop a theoretical understanding of the mechanism of this method of burning rate enhancement and to derive approximate formulae that may be used to obtain estimates of the degree of enhancement. A theoretical analysis containing all essential physical features of the phenomenon has been given previously (Ref. 1); but the author believes that this analysis is somewhat too complicated and not entirely perspicuous. The present study is intended to clarify the nature of the phenomena analyzed in Ref. 1 and to develop simpler working formulae that are, inherently, just as accurate as those of Ref. 1.

In Section II we shall consider a simple problem related to rate-enhanced burning in order to introduce the underlying character of the process. The successful model of rate-enhanced burning is defined and discussed in Section III. In Section IV, what appears to be the simplest conceivable analysis of rate-enhanced burning is presented; a more complete phenomenological theory, which includes all of the physical effects included in the analysis of Ref. 1 but which is less complicated than the analysis of Ref. 1, is presented in Section V.

In Section VI, the predictions of the theory of Section V are discussed and are compared with experiment. Conclusions are given in Section VII.

II. BURNING RATE OF A PROPELLANT SANDWICH

In order to see how the burning rate of a propellant can be modified by placing it adjacent to a substance with a different thermal conductivity, let us consider the simple system illustrated in Fig. 2.1. Two different propellants, each of whose burning rates obey a pyrolysis law, are bonded together. The two propellants will be identified by the subscripts 2 and 3; the subscript 1 identifies conditions in the gaseous phase. Let us assume for simplicity that the specific heats of the solids are constant and equal ($c_2 = c_3 = c$ = constant), that the densities of the solids are constant and equal ($\rho_2 = \rho_3 = \rho$ = constant), and that the thermal conductivities of the solids are constant (λ_2 = constant, λ_3 = constant). Since we are interested in the effect of differing thermal conductivities, we shall assume that $\lambda_2 \neq \lambda_3$. The pyrolysis law governing the burning rate of each propellant will be written as $v_2 = v_2 (T_{1,2})$ and $v_3 = v_3 (T_{1,3})$, where v_2 and v_3 are the normal burning velocities (the linear regression rates) and T_1 is the temperature at the solid-gas interface. We shall seek steady-state solutions for which the motion is in the x direction in Fig. 2.1, the temperature in each solid depends only upon the coordinate normal to the surface of the solid, and the surface of each solid forms an oblique plane (as illustrated in Fig. 2.1).

If v is the velocity of the solid in the x direction, then the normal component of velocity at the surface is $v_2 = v \cos \theta_2$ and $v_3 = v \cos \theta_3$ for solids 2 and 3. Hence,

$$\cos \theta_2 / \cos \theta_3 = v_2 / v_3. \tag{2.1}$$

The solution to the one-dimensional heat conduction equation in a moving medium has been given in the Appendix. Identifying the coordinates η and ζ in the Appendix with our present coordinates x and y, we find that Eq. (A.4) becomes

$$T_2 = A_2 + B_2 \, e^{\mu_2 (x \cos \theta_2 + y \sin \theta_2)} \tag{2.2}$$

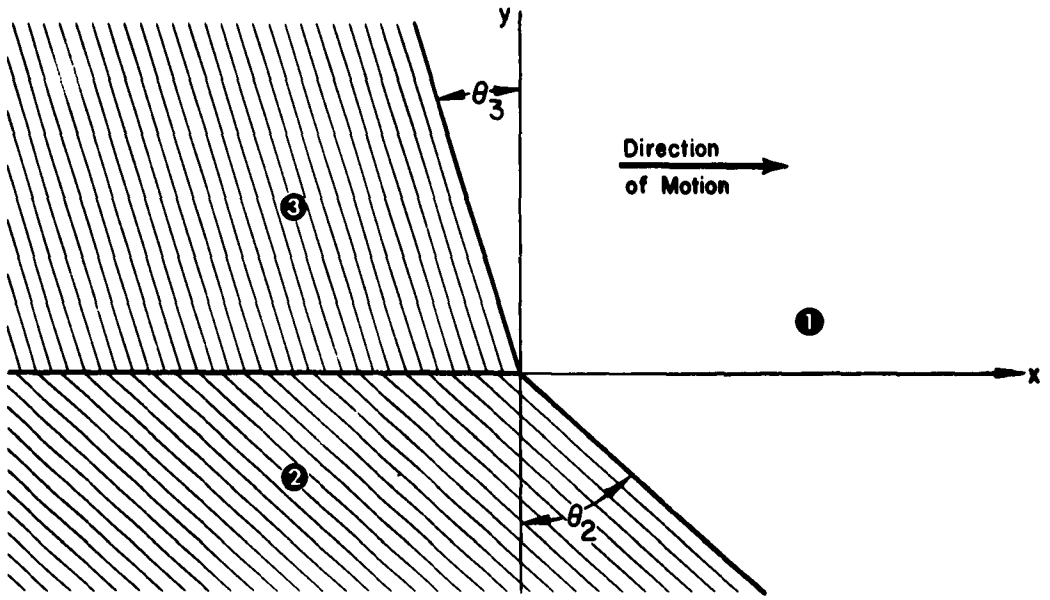

Figure 2.1 MODEL OF TWO PROPELLANTS BONDED TOGETHER

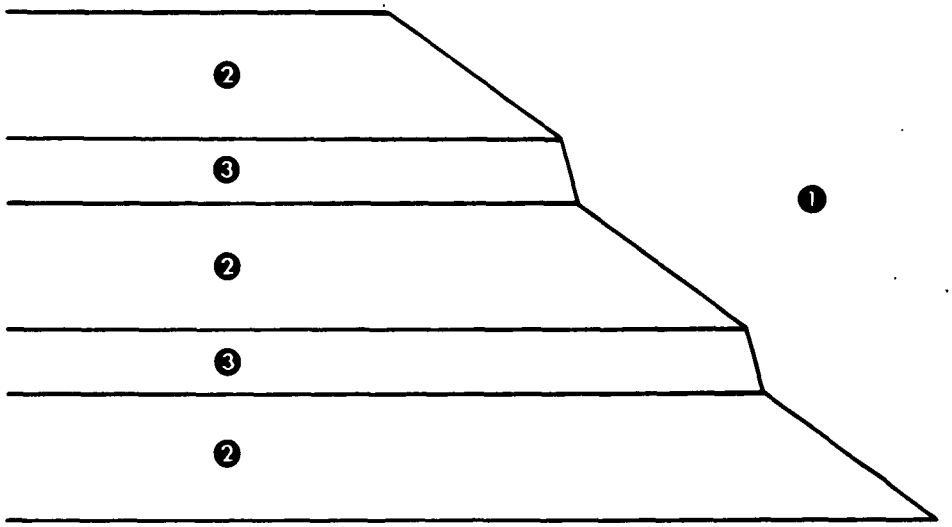

Figure 2.2 SANDWICH PROPELLANT CONSTRUCTION

and

$$T_3 = A_3 + B_3\, e^{\mu_3(x \cos \theta_3 + y \sin \theta_3)} \tag{2.3}$$

in phases 2 and 3, where

$$\mu_2 \equiv \rho\, v \cos \theta_2\, c/\lambda_2 \quad \text{and} \quad \mu_3 \equiv \rho\, v \cos \theta_3\, c/\lambda_3 .$$

Our objective is to find constants A_2, B_2, A_3 and B_3 and angles θ_2 and θ_3 which satisfy Eq. (2.1) and the thermal conditions that must be applied at $x = -\infty$ and along the dividing plane $y = 0$.

As $x \to -\infty$, the temperature in each solid must approach the initial temperature of the propellant, T_o. Hence,

$$A_2 = A_3 = T_o$$

in Eqs. (2.2) and (2.3). Furthermore, the temperatures must be the same in each solid along the plane $y = 0$. This can be true at $x = 0$ only if the interface temperatures are the same ($T_{i,2} = T_{i,3} \equiv T_i$); and it can be true for $x < 0$ only if

$$B_2\, e^{\mu_2 x \cos \theta_2} = B_3\, e^{\mu_3 x \cos \theta_3} \tag{2.4}$$

for all $x < 0$. Equation (2.4) will hold for all $x < 0$ only if

$$B_2 = B_3 = T_i - T_o \text{ and } \mu_2 \cos \theta_2 = \mu_3 \cos \theta_3 .$$

In view of the above relations for μ_2, μ_3, v_2 and v_3, this last condition implies that

$$v_2^2(T_i)/v_3^2(T_i) = \lambda_2/\lambda_3, \tag{2.5}$$

which is a restriction on the physical properties of the propellants. Propellant pairs which do not obey Eq. (2.5) may be expected to have more complicated (non-one-dimensional) temperature fields. For simplicity, we shall consider only propellants for which Eq. (2.5) is

satisfied. Thus, Eqs. (2.2) and (2.3) become

$$T_2 = T_o + (T_1 - T_o)\, e^{\mu_2 \cos \theta_2 \, (x + y \tan \theta_2)} \tag{2.6}$$

and

$$T_3 = T_o + (T_1 - T_o)\, e^{\mu_2 \cos \theta_2 \, (x + y \tan \theta_3)} \, . \tag{2.7}$$

The final thermal boundary condition that the temperature field must satisfy at the plane $y = 0$ is continuity of the normal heat flux (since there are no energy sources located at $y = 0$). This condition can be written as

$$(\lambda \partial T/\partial y)_3 \Big|_{y=0} = (\lambda \partial T/\partial y)_2 \Big|_{y=0} \, .$$

In view of Eqs. (2.6) and (2.7), the condition reduces to

$$\lambda_2 \tan \theta_2 = \lambda_3 \tan \theta_3 \, . \tag{2.8}$$

Equations (2.1) and (2.8) provide two independent relations between the unknown angles θ_2 and θ_3, thereby determining each of these angles. With a little algebra, Eqs. (2.1), (2.5), and (2.8) can be shown to yield

$$v/v_2 = 1/\cos \theta_2 = \sqrt{1 + (\lambda_3/\lambda_2)} \tag{2.9}$$

and

$$v/v_3 = 1/\cos \theta_3 = \sqrt{1 + (\lambda_2/\lambda_3)} \, . \tag{2.10}$$

We have thus obtained unique angles θ_2 and θ_3 such that a simple solution to the heat equation in the solid phases exists. From Eqs. (2.9) and (2.10) it will be noted that, if $\lambda_3 > \lambda_2$, then $\theta_2 > 45^\circ$ and $\theta_3 < 45^\circ$. Also, the composite velocity v is greater than both component normal burning velocities v_2 and v_3. Imbedding propellant 3 with a high thermal conductivity λ_3 in propellant 2 with lower thermal conductivity λ_2 thus increases the burning rate of the original propellant 2. Such a sandwich-type imbedding is illustrated in Fig. 2.2.

III. MODEL OF RATE-ENHANCED BURNING

A reasonable model of rate-enhanced burning that is, algebraically, somewhat complicated has been given in Ref. 1. Qualitative agreement between theory and experiment was obtained. In order to clarify the essential physical characteristics of the process and to obtain more transparent results, it seems to be desirable to analyze a model that is much simpler geometrically but retains the physical phenomena included in Ref. 1. This model is illustrated in Fig. 3.1.

In Fig. 3.1, region 1 is the gaseous phase, region 2 is the solid propellant and region 3 is an inert material (bonded to the propellant) with a high thermal conductivity. A steady-state, two-dimensional system in which all velocities are in the +x direction is implied. The continuity equation is satisfied automatically in this model by the statement that the velocity is a constant, v, in the solid regions (2 and 3) and the velocity is $v\rho_2/\rho_1$ in the gas ($\rho \equiv$ density). Therefore, only the heat equations remain to be considered.

The arrows ($\rightarrow$) in Fig. 3.1 indicate the directions in which heat is supposed to be conducted in the system. An adiabatic (zero heat flow) boundary condition is assumed to be applied along the plane $y = 0$. The inert solid 3 is assumed to be thin enough and of high enough thermal conductivity that the variation in temperature across the material (in the y direction) is negligible; thus, one-dimensional heat conduction (in the x direction), with heat addition from the gas for $x > 0$ and heat rejection to the propellant for $x < 0$, is assumed to occur in region 3. The gaseous reaction zone will be assumed to be so thin that conditions in region 1 can be assumed to be practically uniform and the temperature T_1 can be assumed to be approximately equal to the adiabatic flame temperature T_∞. Actually, the higher velocity in the gas, caused by the lower density of the gas (see Fig. 3.2), leads to boundary layer development (indicated by the dashed lines in region 1 in Fig. 3.1) on the solid surfaces. The burning surface between regions 1 and 2 will be assumed to be a

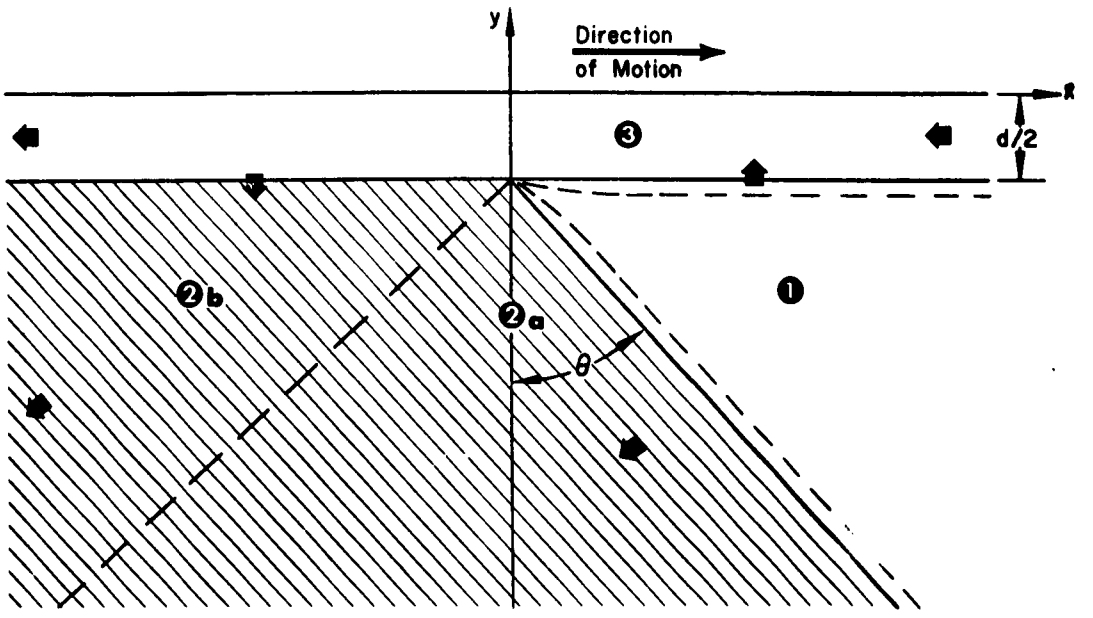

Figure 3.1 MODEL OF RATE-ENHANCED BURNING

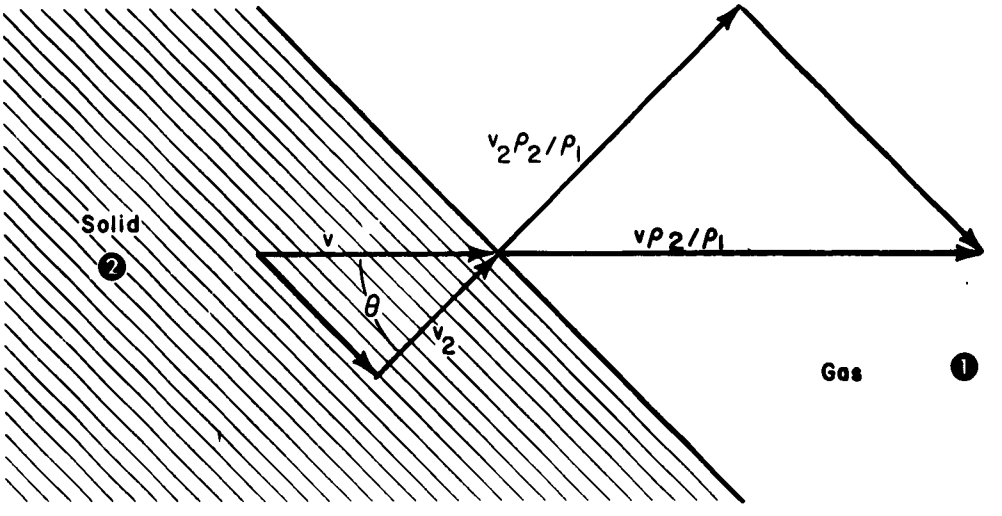

Figure 3.2 VELOCITY VECTOR DIAGRAMS IN THE GAS AND IN THE SOLID PROPELLANT.

plane. Therefore, the normal linear regression rate of the surface is constant. Since we are considering propellants obeying a pyrolysis law, this implies that the surface is an isotherm; i.e., the surface temperature T_1 is constant. The temperatures in both regions 2 and 3 approach the initial temperature T_o as $x \to -\infty$. At sufficiently large values of y, the solid propellant will experience one-dimensional heat conduction in a direction normal to its surface, and the temperature profile will be unaffected by the presence of material 3; [the only influence is the superimposed transverse velocity (parallel to the surface) illustrated in Fig. 3.2]. We shall assume that this condition holds throughout region 2a (divided from region 2b by the dashed line normal to the propellant surface in Fig. 3.1). The energy required to heat up region 2b is assumed to be supplied by heat conduction from material 3.

The model in Fig. 3.1 will also be applicable to axially-symmetrical systems (e.g., when x is an axis of symmetry, region 3 is a cylindrical wire and the propellant surface is conical) provided the thickness of the thermal boundary layers (i.e., the distances required for T to become practically equal to either T_∞ or T_o) in regions 1 and 2 are small compared to the radius of region 3; numerical estimates indicate that this is often true for wires greater than .001 inches in diameter.

Consideration of the temperature field and of the heat transfer processes should determine the angle θ in Fig. 3.1. This provides the fractional increase in the burning velocity, since

$$v/v_2 = 1/\cos\theta \qquad (3.1)$$

(see Fig. 3.2; $v_2 \equiv$ normal burning velocity of the propellant 2).

IV. SIMPLE TEMPERATURE MATCHING

In order to obtain a quick and simple (although inaccurate) indication of how the heat flow processes can determine θ, let us employ the following approximate intuitive criterion: Along the plane dividing regions 2 and 3, the temperature in medium 3 must drop to T_o in

approximately the same distance that the temperature in medium 2 drops to T_o. A gross violation of this rule would lead to inordinately large rates of heat transfer between materials 2 and 3 in a region where the temperature of one of these materials is practically uniform.

An estimate of the distance required for the temperature to approach T_o may be obtained from Eq. (A.3), from which it can be seen that a characteristic decay length (in the direction in which the temperature varies) for the temperature profile in a moving medium is $1/\mu$. In the propellant, the value of μ (in the direction normal to the surface) is

$$\mu_2 = \rho_2 \, v_2 \, c_2/\lambda_2 = \rho_2 \, v \cos\theta \, c_2/\lambda_2 , \qquad (4.1)$$

($c \equiv$ specific heat capacity and $\lambda \equiv$ thermal conductivity). Since $\cos\theta = 0$ in the inert material 3 (i.e., the temperature is uniform in planes normal to the x axis),

$$\mu_3 = \rho_3 \, v_3 \, c_3/\lambda_3 = \rho_3 \, v \, c_3/\lambda_3 . \qquad (4.2)$$

The geometrical construction shown in Fig. 4.1 implies that the temperature matching condition is

$$(1/\mu_3) \cos\theta = 1/\mu_2 . \qquad (4.3)$$

Equations (4.1) through (4.3) yield

$$1/\cos\theta = \sqrt{(\rho_2 \, c_2/\lambda_2)/(\rho_3 \, c_3/\lambda_3)} \quad . \qquad (4.4)$$

The principal result exhibited by Eq. (4.4) is the relationship

$$1/\cos\theta \sim \sqrt{\lambda_3/\lambda_2} \; ; \qquad (4.5)$$

the fractional increase in the burning rate is proportional to the square root of the thermal conductivity of material 3. Essentially this same result is obtained with practically every reasonable model of the process, and rough experimental confirmation of this result has been obtained.[1] However, Eq. (4.4) does not predict the observed dependence of $1/\cos\theta$ upon the thickness $d/2$ of medium 3. An improved version of

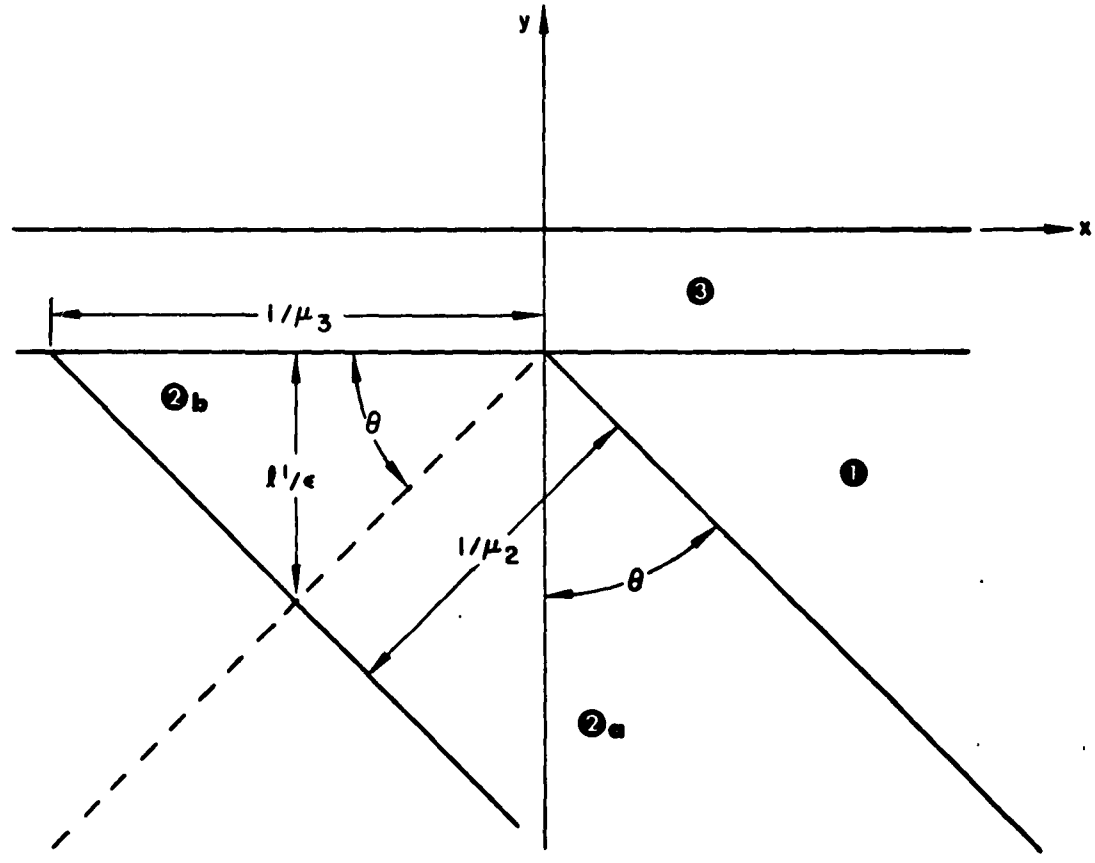

Figure 4.1 GEOMETRY OF SIMPLE TEMPERATURE MATCHING

the temperature-matching theory, given below, does, however, yield a thickness dependence.

Equation (A.3) really isn't applicable to medium 3 because, as indicated in Fig. 3.1, heat is being lost from medium 3 through heat conduction to medium 2. The temperature of medium 3 therefore drops to T_o in a distance that is shorter than $1/\mu_3$, with μ_3 given by Eq. (4.2). An estimate of the decay length, accounting for this heat loss, may be obtained from Eq. (A.7).

Let us assume that the rate of heat loss is proportional to $T - T_o$. Then $T_R = T_o$ in Eq. (A.7). Since $\mu' > 0$, $\kappa' > 0$ and $T \to T_o$ as $x \to -\infty$, we must have $b = 0$ in region 3 for $x < 0$. Hence, in region 3 for $x < 0$, $T - T_o \sim e^{\left[1 + \sqrt{1 + \kappa'}\right] \mu' x/2}$ according to Eq. (A.7). This implies that the characteristic decay length in medium 3 is

$$(2/\mu') \left[1 + \sqrt{1 + \kappa'}\right]^{-1} ,$$

where μ' and κ', defined in the Appendix, refer to region 3. Using these definitions, we find that our previous temperature matching condition becomes

$$\left[2/(\rho_3 \, v_3 \, c_3/\lambda_3)\right]\left[1 + \sqrt{1 + (4K/\lambda_3)/(\rho_3 \, v_3 \, c_3/\lambda_3)^2}\right]^{-1} \cos\theta = 1/(\rho_2 \, v_2 \, c_2/\lambda_2) .$$

Since $v_3 = v = v_2/\cos\theta$, where v_2 is the normal linear regression rate of the propellant, this formula can be written as

$$\cos^2\theta = \frac{1}{2}\left(\frac{\rho_3 \, c_3/\lambda_3}{\rho_2 \, c_2/\lambda_2}\right)\left\{1 + \sqrt{1 + \left[4K \, \lambda_3/(\rho_3 \, v_2 \, c_3)^2\right]\cos^2\theta}\right\} \qquad (4.6)$$

where

$$4K \, \lambda_3/(\rho_3 \, v_2 \, c_3)^2 = \kappa'/\cos^2\theta$$

is independent of θ. Equation (4.6) can easily be solved explicitly for $\cos^2\theta$; the result yields

$$1/\cos\theta = \sqrt{\frac{\rho_2\, c_2/\lambda_2}{\rho_3\, c_3/\lambda_3}}\left[1 + \frac{K\,\lambda_3}{c_2\, c_3\, \rho_2\, \rho_3\, v_2^2}\right]^{-1/2} . \quad (4.7)$$

Equation (4.7) is the same as Eq. (4.4) except for the heat-loss correction term appearing inside the square brackets. This heat loss is seen to reduce the fractional increase in the burning rate ($1/\cos\theta$). Furthermore, the correction term has no explicit dependence upon λ_3; the λ_3 dependence given by Eq. (4.5) remains valid. In order to show that the correction term depends upon the thickness of region 3, we must obtain an estimate of the heat loss constant K.

Since the heat loss from material 3 occurs by conduction into material 2, the energy per unit surface area per second lost from medium 3 is approximately

$$\lambda_2\,(T - T_o)/\ell,$$

where ℓ is a representative heat conduction length in medium 2. The energy lost per unit volume per second is therefore

$$K(T - T_o) = \lambda_2\left(\frac{T - T_o}{\ell}\right)\left(\frac{\text{surface area}}{\text{volume}}\right) = \begin{cases} [\lambda_2(T - T_o)/\ell]\ (2/d) & \text{for plane geometry} \\ [\lambda_2(T - T_o)/\ell]\ (4/d) & \text{for cylindrical geometry} \end{cases} .$$

Hence,

$$K = (4\lambda_2)/(\ell_{\text{eff}}\, d), \quad (4.8)$$

where ℓ_{eff} may be termed an effective heat conduction length and d is either the diameter or the thickness of region 3, depending upon whether region 3 is a cylinder or a slab. As a very rough estimate, we may set ℓ_{eff} equal to the decay length in region 2, viz., $1/\mu_2$, thereby obtaining

$$K \approx 4\, c_2\, \rho_2\, v_2/d \quad (4.9)$$

[see Eq. (4.1)] and reducing Eq. (4.7) to

$$1/\cos\theta \approx \sqrt{\frac{\rho_2\ c_2/\lambda_2}{\rho_3\ c_3/\lambda_3}}\left[1 + \frac{4\ \lambda_2}{c_3\ \rho_3\ v_2\ d}\right]^{-1/2}. \qquad (4.10)$$

It is clear from Eq. (4.8) that K depends upon the thickness d; viz., $K \sim 1/d$. Increasing d decreases K and therefore increases the fractional enhancement in the burning rate $1/\cos\theta$. The quantity $1/\cos\theta$ approaches its maximum value, given by Eq. (4.4), as $d \to \infty$. The present formulae therefore do not predict the observed[1] existance of an optimum d and the observed decrease in $1/\cos\theta$ with increasing d above this optimum thickness. The formulae developed in the following section do exhibit these refinements. Equation (4.10) predicts that the dependence of $1/\cos\theta$ upon d enters through the product v_2 d. This result is also predicted by the theory developed in the following section and is roughly confirmed by experiment.[1]

V. PHENOMENOLOGICAL THEORY

In order to develop a treatment that might possibly be termed a "theory", let us replace the temperature matching condition by an energy balance. Suppose that the temperature profiles (along a line normal to the propellant surface) in region 2 a of Fig. 3.1 differ negligibly from those in a propellant burning normally. Then no heat is transferred across the dashed line separating regions 2 a and 2 b in Fig. 3.1. All of the energy required to heat up the material in region 2 b must therefore be supplied by conduction from region 3. Heat enters region 3 only through heat transfer from the gas in the region $x > 0$. An overall energy balance for region 3 therefore states that the energy entering region 3 in $x > 0$ must equal the sum of the energies required to heat up regions 2 b and 3.

Let us consider a slab geometry of unit height (normal to the paper in Fig. 3.1). The energy per second required to heat up region 3 then becomes

$$E_3 = c_3 (T_\infty - T_o) \rho_3 v_3 d/2 = \rho_3 c_3 (T_\infty - T_o) v_2 d/(2 \cos \theta), \quad (5.1)$$

where the adiabatic flame temperature T_∞ is the temperature approached in medium 3 as $x \to \infty$.

A close estimate of the energy required to heat up region 2 b may be obtained by assuming that the temperature profile along the dashed line bounding region 2 b differs little from that in region 2 a [i.e., is given by Eq. (A.3)]. If ξ is the coordinate normal to the propellant surface in Fig. 3.1, then (since $T = T_1$, the surface temperature, at $\xi = 0$ and $T \to T_o$ as $\xi \to -\infty$) Eq. (A.3) becomes

$$T = T_o + (T_1 - T_o) e^{\mu_2 \xi} . \quad (5.2)$$

The excess energy flux in region 2 b is $\rho_2 v c_2 (T - T_o)$, and the component of this flux vector normal to the dashed line in Fig. 3.1 is $\rho_2 v c_2 (T - T_o) \sin \theta$. The energy per second required to heat up the material in region 2 b is therefore

$$E_2 = \int_{\text{bdry}} (\text{normal flux})\, d(\text{area}) = \int_{-\infty}^{0} \rho_2 v c_2 (T - T_o) \sin \theta \, d\xi . \quad (5.3)$$

Substituting Eq. (5.2) into Eq. (5.3) and integrating yields

$$E_2 = \lambda_2 (T_1 - T_o) \tan \theta , \quad (5.4)$$

where use has been made of Eq. (4.1) for μ_2.

The energy per second added to material 3 from the gas can be related to the appropriate heat transfer coefficient h; the energy per unit surface area per second added to medium 3 is $h (T_\infty - T)$, where T_∞ is the temperature of the gas and T is the local temperature in medium 3. The temperature distribution in region 3 for $x > 0$ can be obtained from Eq. (A.7). Here $T_R = T_\infty$, and, since $T \to T_\infty$ as $x \to \infty$, we must have $a = 0$. If T_Z denotes the value of T in region 3 at $x = 0$, then Eq. (A.7) becomes

$$T = T_\infty - (T_\infty - T_Z)\, e^{\left[1 - \sqrt{1 + \kappa'}\right]\mu' x/2} . \qquad (5.5)$$

The quantities μ' and κ' (which here refer to material 3) are defined in the Appendix; the value of K appearing in the definition of κ' is seen geometrically to be related to the heat transfer coefficient through the formula

$$K = h(2/d) \qquad (5.6)$$

for our present slab geometry. The total energy per second added to region 3 is

$$E_1 = \int_0^\infty h\,(T_\infty - T)\, dx , \qquad (5.7)$$

where T is given by Eq. (5.5). Assuming that h is independent of x, we find by evaluating the integral in Eq. (5.6) that

$$E_1 = h(T_\infty - T_Z)\,(2/\mu')\left[\sqrt{1 + \kappa'} - 1\right]^{-1}$$

$$= h(T_\infty - T_Z)\,\frac{2\lambda_3 \cos\theta}{c_3 \rho_3 v_2}\left[\sqrt{1 + \frac{8h\,\lambda_3 \cos^2\theta}{d c_3^2 \rho_3^2 v_2^2}} - 1\right]^{-1} . \qquad (5.8)$$

The energy balance stated previously may be written as

$$E_1 = E_2 + E_3 , \qquad (5.9)$$

where E_1 is given by Eq. (5.8), E_2 is given by Eq. (5.4), and E_3 is given by Eq. (5.1). Besides the angle θ, the only unknown parameter appearing in any of these equations is the temperature T_Z.

In order to relate T_Z to θ, we may employ the condition that the energy to heat up region 2 b is obtained by thermal conduction from region 3. An estimate of the amount of heat conducted out of medium 3 in the region $x < 0$ can be obtained in terms of a heat transfer coefficient h', defined in such a way that the energy per unit area per second

leaving medium 3 is $h'(T - T_o)$, where T is the temperature in medium 3. If we assume that h' is independent of x, then Eq. (A.7) with $T_R = T_o$ determines T(x) in medium 3 for $x < 0$. Since $T = T_o$ at $x = -\infty$ and $T = T_Z$ at $x = 0$, we find that $b = 0$ and $a = (T_Z - T_o)$. Therefore the total energy per second leaving medium 3 is

$$\int_{-\infty}^{x} h'(T_Z - T_o)\, e^{\left[1 + \sqrt{1+\kappa'}\right]\mu' x/2}\, dx = h'(T_Z - T_o)\,(2/\mu')\left[1+\sqrt{1+\kappa'}\right]^{-1}.$$

Since this heat flow rate must be equal to E_2, we obtain (employing the definitions of μ' and κ' and the relation between K and h')

$$E_2 = h'(T_Z - T_o)\,\frac{2\lambda_3 \cos\theta}{c_3\,\rho_3\,v_2}\left[1 + \sqrt{1 + \frac{8h'\lambda_3\cos^2\theta}{d c_3^2\,\rho_3^2\,v_2^2}}\right]^{-1}. \qquad (5.10)$$

An estimate of h' is $h' = \lambda_2/\ell'$, where ℓ' is a representative heat conduction length in region 2 b. It may be reasonable to assume that ℓ' is proportional to the distance indicated in Fig. 4.1; hence, let us set $\ell' = \epsilon \sin\theta\, \lambda_2/(\rho_2\, v_2\, c_2)$, where the coefficient ϵ is assumed to be independent of all experimentally variable parameters. Equation (5.10) then reduces to

$$E_2 = (T_Z - T_o)\left(\frac{c_2\,\rho_2}{c_3\,\rho_3}\right)\frac{2\lambda_3\cos\theta}{\epsilon\sin\theta}\left[1 + \sqrt{1 + \frac{8\,\rho_2\,c_2\,\lambda_3\cos^2\theta}{d\,c_3^2\,\rho_3^2\,v_2\,\epsilon\sin\theta}}\right]^{-1}. \qquad (5.11)$$

Equations (5.1), (5.4), (5.8), (5.9) and (5.11) serve to determine θ.

If we introduce Eq. (5.4) into Eq. (5.11), solve for $(T_\infty - T_Z)$, and substitute the result into Eq. (5.8), we find that

$$E_1 = \frac{h(T_\infty - T_o)\,\dfrac{2\lambda_3\cos\theta}{c_3\,\rho_3\,v_2}}{\sqrt{1+\dfrac{8h\lambda_3\cos^2\theta}{dc_3^2\,\rho_3^2\,v_2^2}} - 1}\left\{1 - \left(\frac{T_i - T_o}{T_\infty - T_o}\right)\left(\frac{c_3\,\rho_3/\lambda_3}{c_2\,\rho_2/\lambda_2}\right)\frac{\epsilon}{2}\tan^2\theta \cdot \left[1 + \sqrt{1+\frac{8\rho_2\,c_2\,\lambda_3\cos^2\theta}{dc_3^2\,\rho_3^2\,v_2\,\epsilon\sin\theta}}\right]\right\}. \qquad (5.12)$$

Let us introduce the dimensionless variables

$$\alpha \equiv (\rho_2\ c_2/\lambda_2)/(\rho_3\ c_3/\lambda_3) \tag{5.13}$$

[a measure of λ_3],

$$\gamma \equiv (\rho_3\ c_3)/(\rho_2\ c_2), \tag{5.14}$$

[a measure of c_3],

$$\delta \equiv d\ \rho_2\ v_2\ c_2/\lambda_2, \tag{5.15}$$

[a measure of d],

$$\tau \equiv (T_i - T_o)/(T_\infty - T_o) \tag{5.16}$$

and

$$H \equiv h\ d/\lambda_2\ . \tag{5.17}$$

When Eqs. (5.1), (5.4) and (5.12) are substituted into Eq. (5.9), we find, in terms of these dimensionless variables,

$$\frac{H\alpha}{\delta}\ 2\ \cos\theta \left\{1 - \frac{\tau\epsilon}{2\alpha}\tan^2\theta \left[1 + \sqrt{1 + \frac{8\alpha\ \cos^2\theta}{\delta\ \gamma\ \epsilon\ \sin\theta}}\right]\right\}$$
$$= \left[\sqrt{1 + \frac{8H\ \alpha\ \cos^2\theta}{\delta^2\ \gamma}} - 1\right] \left[\tau\ \tan\theta + \frac{\gamma\ \delta}{2\ \cos\theta}\right]\ . \tag{5.18}$$

Equation (5.18) is expected to determine θ in terms of known parameters.

In order to use Eq. (5.18) to compute θ, it is necessary to know the heat transfer coefficient h so that H may be related to θ, δ, etc. In the plane two-dimensional system presently under consideration, heat is transferred from the gas to medium 3 by convection through a flat-plate boundary layer. The quantity h is then proportional to the ratio

of λ_1 (the thermal conductivity of the gas) to the thickness of the boundary layer. The boundary layer thickness is, in turn, proportional to $x/\sqrt{Re}$, where $Re = \rho_1 (v_1 - v) x/\eta_1$ is the local Reynolds number, (ρ_1 = density of the gas, v_1 = velocity of the gas, η_1 = coefficient of viscosity for the gas). Since mass conservation shows that $v/v_1 = \rho_1/\rho_2$, we find

$$h \approx \frac{\lambda_1}{x} \sqrt{\frac{\rho_2 \, v_2 \, x}{\eta_1 \cos \theta} \left(1 - \frac{\rho_1}{\rho_2}\right)} .$$

The appropriate average value for x in this expression is $(2/\mu') \left[\sqrt{1 + \kappa'} - 1\right]^{-1}$ according to Eq. (5.5). Substituting the above expression into Eq. (5.17) and utilizing Eq. (5.15) yields

$$H \approx \delta \left[\left(\frac{\lambda_1^2}{\eta_1 \, c_2^2 \, \rho_2 \, v_2 \, x} \right) \frac{1 - (\rho_1/\rho_2)}{\cos \theta} \right]^{1/2} , \qquad (5.19)$$

which shows that the δ and θ dependence of H is determined by $H \sim \delta (x \cos \theta)^{-1/2}$. The explicit dependence of H upon $\cos \theta$, δ, etc., can be unraveled by substituting the previously given expression for the average value of x, viz.,

$$x \approx \frac{2\lambda_s \cos \theta}{c_s \rho_s v_2} \left[\sqrt{1 + \frac{8H \alpha \cos^2 \theta}{\delta^2 \gamma}} - 1 \right]^{-1} , \qquad (5.20)$$

into Eq. (5.19) and solving for H.

Of greater practical interest is the cylindrically symmetrical system. It can be shown that, provided the thickness of the thermal boundary layer in the propellant (region 2) is small compared with the diameter of region 3, the only modifications in our previous development are that an additional factor of 1/2 appears in the expression for E_s [on the right-hand side of Eq. (5.1)] and that an additional factor of 2 appears in the numerator on the right-hand side of Eq. (5.6). This last modification leads to an additional factor of 2 in the numerator inside the radical sign in Eqs. (5.8) and (5.11), thus causing the coefficient 8 to be replaced by 16 inside both radical signs in Eq. (5.18).

The first modification causes the factor 1/2 to be replaced by 1/4 in the last term in Eq. (5.18).

The expression for n (and therefore for H) in the cylindrically symmetrical case is the same as that given above for the plane case, provided the thickness of the gaseous boundary layer on medium 3 is small compared with the diameter of medium 3 throughout the region in which appreciable heat transfer from medium 1 to medium 3 occurs. Numerical estimates indicate that this condition will be satisfied for d ~ a few thousandths of an inch provided x [as estimated from Eq. (5.20)] is less than roughly 1 cm. Since a direct estimate of x from Eq. (5.20) yields x ~ a few cm., the validity of the above condition is questionable, and it may be better to employ empirical formulae for h for small wires placed parallel to the flow direction. Jacob[2] quotes results of this type obtained by Muhler in turbulent flow with the Reynolds number based upon wire diameter, Re_d, in our present range of interest ($40 \lesssim Re_d \lesssim 4000$); these results have also been corroborated (in a close approximation) by some very recent work. The results quoted by Jacob may be correlated roughly by the formula Nusselt number = $hd/\lambda_1 \approx .3\ Re_d^{.47}$, a reasonable and convenient approximation to which is

$$h = .25\ (\lambda_1/d)\left[\rho_1(v_1 - v)\ d/\eta_1\right]^{.5} . \qquad (5.21)$$

Since $\rho_1 << \rho_2$, we have $v << v_1$, and Eq. (5.21) can be written as

$$H = \beta\ \delta^{.5}/\cos^{.5}\theta, \qquad (5.22)$$

where

$$\beta \equiv .25 \left(\frac{\lambda_1}{\lambda_2}\right)\left(\frac{\lambda_2/c_2}{\eta_1}\right)^{.5} \qquad (5.23)$$

and use has been made of Eqs. (5.15) and (5.17) and of the identity $\rho_1\ v_1 = \rho_2\ v = \rho_2\ v_2/\cos\theta$. Although the accuracy inherent in Eq. (5.22) is not great, this relation does provide a useful order-of-magnitude estimate, and it appears to be as accurate an expression

as one can obtain for a flow system in which the geometry is as complicated as that presently under consideration.

By substituting Eq. (5.22) into Eq. (5.18) and also introducing the other modifications (indicated above) that arise in Eq. (5.18) for cylindrical geometry, we obtain

$$\frac{2\alpha\beta\cos^{1.5}\theta}{\sqrt{\delta}}\left\{1-\frac{\tau\epsilon}{2\alpha}\tan^2\theta\left[1+\sqrt{1+\frac{16\alpha\cos^2\theta}{\delta\gamma\epsilon\sin\theta}}\right]\right\}$$

$$=\left[\sqrt{1+\frac{16\alpha\beta\cos^{1.5}\theta}{\gamma\delta^{1.5}}}-1\right]\left[\tau\sin\theta+\frac{\gamma\delta}{4}\right] \quad . \qquad (5.24)$$

Solution of Eq. (5.24) (by trial and error) for the value of θ corresponding to prescribed values of α, β, γ, δ, ϵ and τ determines the fractional enhancement in the burning rate. In subsequent sections we shall consider only cylindrically symmetrical systems, employing Eq. (5.24) instead of Eq. (5.18).

VI. RESULTS AND COMPARISON WITH EXPERIMENT

One very general consequence of Eq. (5.24) is that the dependence of θ upon both d and v_2 enters only through the parameter δ; i.e., α, β, γ, ϵ and τ are all independent of both d and v_2 [see Eqs. (5.13), (5.14), (5.16) and (5.23)]. This result actually does not even depend upon the heat transfer assumptions associated with the cylindrical geometry since Eqs. (5.18) through (5.20) can be shown to yield the same result for plane geometry. In view of the definition of δ [Eq. (5.15)], we may conclude that θ is a function of the product dv_2 when all other parameters are held fixed. The normal linear regression rate v_2 can be varied practically independently of all other parameters appearing in our formulae by varying the chamber pressure. Experimental data on the effect of varying both d and v_2 independently is therefore available.[1] A plot of $1/\cos\theta$ vs. dv_2 for various values of v_2, obtained from the experimental data, is shown in Fig. 6.1. A small systematic influence of v_2 is noticeable, thus indicating that the foundations of our theory are not entirely applicable to these experiments. In extreme cases

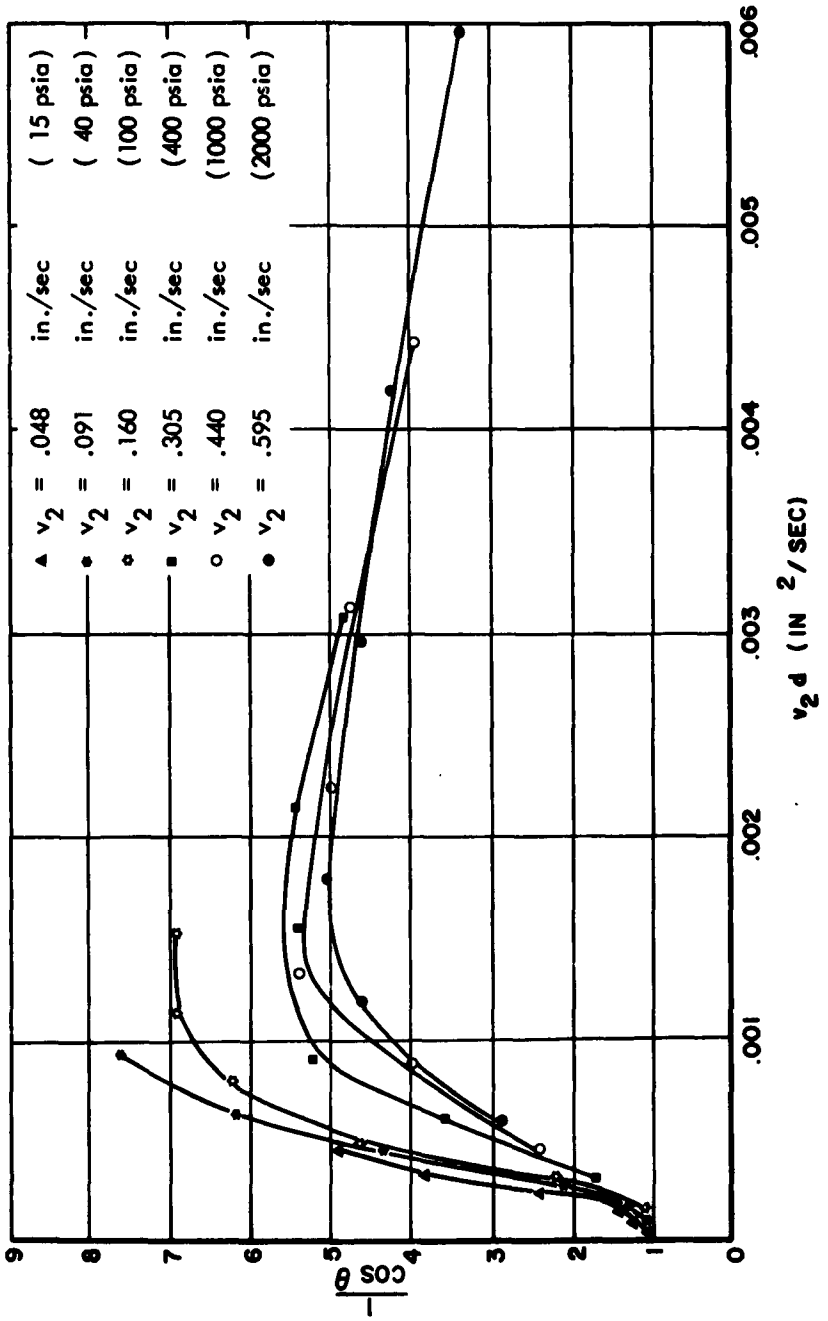

Figure 6.1 – The ratio of the enhanced burning rate to the normal burning rate as a function of the product of the normal burning rate and the diameter, computed from the experimental data of reference 1.

(near the peak value of $1/\cos\theta$), the discrepancy is seen to amount to nearly a factor of 2 in $1/\cos\theta$ for given dv_2. This same objection may be raised against the more complicated theory of Ref. 1. There are a number of possible causes of the discrepancy; for example, we did not consider the fact that if the number of wires and the chamber size remain fixed as the wire diameter is increased, then the over-all adiabatic flame temperature decreases as d increases. Our primary reason for emphasizing this discrepancy is to illustrate that the present theory cannot reasonably be expected to yield enhanced burning rates that will agree with ordinary experiments more closely than a factor of 2.

Various general characteristics of Eq. (5.24) are of interest. For example, it can be seen that, as $\delta \to 0$, the factor in the curly brackets in Eq. (5.24) must vanish, and Eq. (5.24) therefore yields

$$\frac{1}{\cos\theta} - 1 = \frac{1}{2}\left(\frac{\alpha\gamma\delta}{4\epsilon\tau^2}\right)^{2/3} \tag{6.1}$$

for very small values of δ. It can also be shown from Eq. (5.24) that, as $\delta \to \infty$, $\cos\theta$ again approaches unity; explicitly,

$$\frac{1}{\cos\theta} - 1 = \left(\frac{\alpha^2\beta}{8\gamma\epsilon\tau}\right)\delta^{-3/2} \tag{6.2}$$

for very large values of δ. To obtain Eq. (6.2) involves retaining a three-term expansion of the radical on the right-hand side of Eq. (5.24). Since $\frac{1}{\cos\theta} \to 1$ as $\delta \to 0$ and as $\delta \to \infty$, we conclude that $1/\cos\theta$ attains at least one maximum value for positive δ. The quantity $1/\cos\theta$ is bounded for all $\delta \geq 0$ because the quantity in the curly brackets in Eq. (5.24) must remain non-negative; setting the curly bracket equal to zero yields

$$\left(\frac{\alpha}{\tau\epsilon} + 1\right)\cos^2\theta - 1 = \left(\frac{4\tau}{\gamma\delta}\right)(1 - \cos^2\theta)^{3/2} \tag{6.3}$$

(providing a cubic equation for the minimum value of $\cos^2\theta$), thus implying that

$$1/\cos\theta \leq \sqrt{\frac{\alpha}{\tau\epsilon} + 1} \qquad (6.4)$$

for all $\delta \geq 0$ [since the right-hand side of Eq. (6.3) is non-negative]. The maximum value of $1/\cos\theta$ must therefore be finite. Equation (6.4) shows that the bound on the fractional increase in the burning rate is proportional to $\sqrt{\alpha}$ [i.e., proportional to $\sqrt{\lambda_g/\lambda_s}$; see Eq. (5.13)] for the physically important range of values of the parameters (viz., for $\alpha/\tau\epsilon \gtrsim 10^3$); this result has already been suggested in Section IV [see Eq. (4.5)] and, as has previously been indicated, is in rough agreement with experiment.

The value of $1/\cos\theta$ as a function of δ, obtained from Eq. (5.24) for the representative case $\alpha = 10^3$, $\beta = 10^{-1}$, $\gamma = 1$, $\epsilon = 1$, $\tau = 1$, is plotted in Fig. 6.2. The values of δ in the experiments reported in Ref. 1 lie between 1 and 50. Comparison of Figs. 6.1 and 6.2 indicates qualitative agreement between theory and experiment. The order of magnitude of the maximum enhancement in the burning rate is the same on the theoretical and experimental curves. The largest difference between theory and experiment appears to occur at small values of δ and can be reduced considerably by suitably adjusting the values of γ, ϵ and τ.

VII. CONCLUSIONS

The model given in Section III and the analysis given in Section V appear to explain the underlying physical mechanism of rate-enhanced burning. The principal result of this study is Eq. (5.24), which determines the burning rate as a function of the physical parameters of the problem. The primary qualitative conclusion is that the ratio of the enhanced burning rate to the normal burning rate is proportional to the square root of the ratio of the thermal conductivity of the wire to that of the propellant (i.e., to $\sqrt{\alpha}$). For ordinary materials, this square root does not exceed about 50, and, when the correct constant of proportionality is employed, it is found that the burning rate can be increased at most by a factor of 10. It may also be noted [see, for example, Eq. (6.4)] that a small value of τ (i.e., a small ratio of the

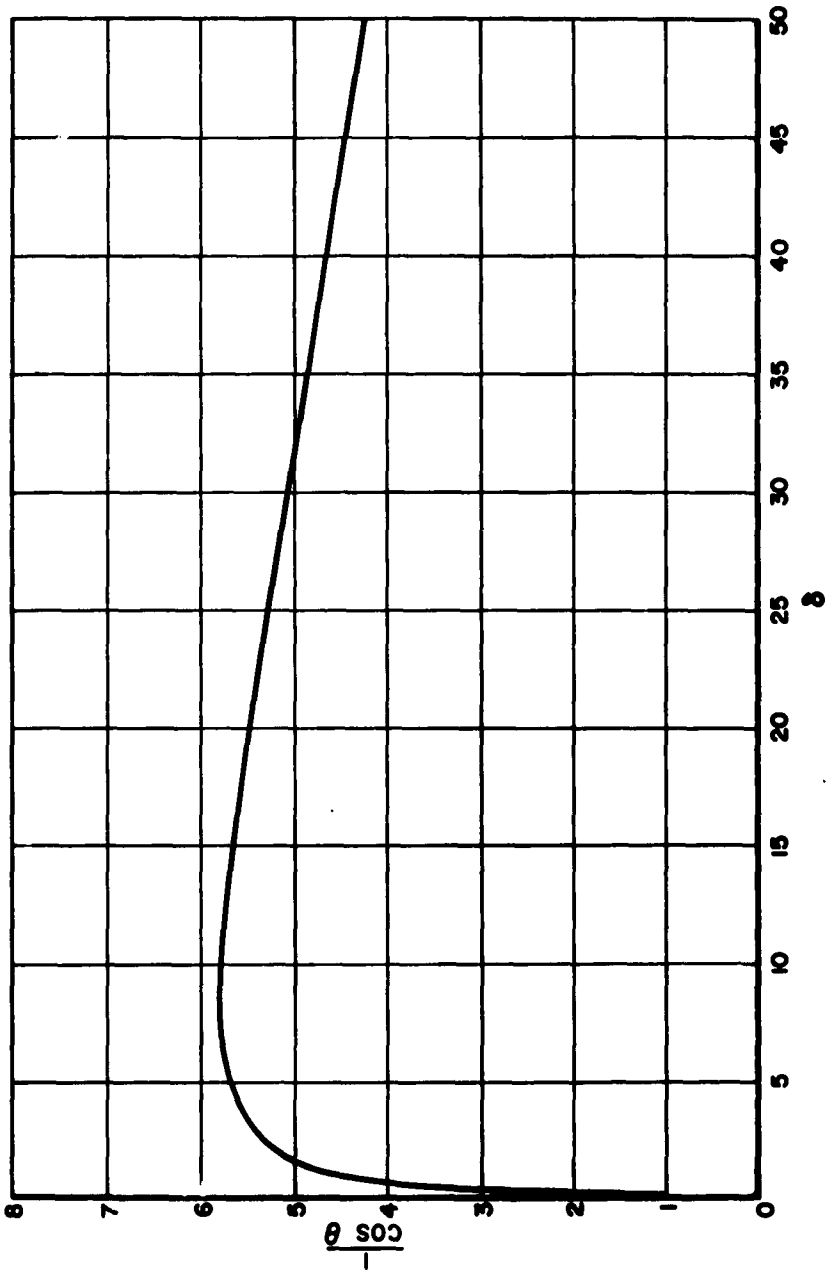

Figure 6.2 – The ratio of the enhanced burning rate to the normal burning rate as a function of the dimensionless diameter δ, computed from eq. (5.24), for $\alpha = 10^{3}$, $\beta = 10^{-1}$, $\gamma = 1$, $\epsilon = 1$, $\tau = 1$.

propellant surface temperature to the adiabatic flame temperature) favors a larger relative increase in the burning rate.

There are many related basic research problems that appear to be interesting. For example, an analysis of steady-state, reacting, flat-plate boundary layer flow, with a solid phase located upstream (at the forward edge of the plate) and with the plate moving slowly in the flow direction, would appear to be tractable (although perhaps difficult) and would represent the flow in the vertex where the propellant meets the wire. However, no analyses of this type are essential for predicting the degree of enhancement of the burning rate; the controlling physical mechanism of rate-enhanced burning is now well-understood.

APPENDIX

SOLUTIONS OF THE STEADY-STATE ONE-DIMENSIONAL HEAT CONDUCTION EQUATION IN A MOVING SOLID

Let us consider a material for which the density ρ, the heat capacity c and the thermal conductivity λ are all constant. If this material is moving with velocity $\vec{v}$, then, in the absence of heat sources or sinks, the steady-state differential equation governing the distribution of the temperature T in the material becomes

$$c \rho \vec{v} \cdot \nabla T - \lambda \nabla^2 T = 0 . \qquad \text{(A.1)}$$

For a non-rotating solid body, $\vec{v}$ is constant everywhere; i.e.,

$$\vec{v} = v \vec{e}_\eta ,$$

where v is the (constant) magnitude of the velocity and $\vec{e}_\eta$ is a unit vector in the $\vec{v}$ direction. Let us investigate systems in which the temperature is a function only of a single cartesian coordinate ξ. If $\vec{e}_\xi$ denotes a unit vector in the ξ direction, then Eq. (A.1) reduces to

$$(c \rho v/\lambda) (\vec{e}_\eta \cdot \vec{e}_\xi) \, dT/d\xi - d^2T/d\xi^2 = 0 . \qquad \text{(A.2)}$$

The dot product appearing in Eq. (A.2) is simply

$$\vec{e}_\eta \cdot \vec{e}_\xi = \cos \theta ,$$

where θ is the angle between the ξ and η directions. It may be noted that the component of $\vec{v}$ in the ξ direction is

$$\vec{v} \cdot \vec{e}_\xi = v \cos \theta \equiv v_\xi .$$

We shall assume that $\cos\theta \neq 0$ and shall define a characteristic length $1/\mu$ by

$$\mu \equiv \rho\, v \cos\theta\, c/\lambda.$$

The general solution to Eq. (A.2) then becomes

$$T = A + B\, e^{\mu\xi}, \tag{A.3}$$

where A and B are arbitrary constants. In the plane containing $\vec{e}_\xi$ and $\vec{e}_\eta$ we may introduce the cartesian coordinate system illustrated in Fig. A.1; [$\vec{e}_\zeta$ is normal to $\vec{e}_\eta$ and $\xi = \eta \cos\theta + \zeta \sin\theta$]. In terms of the coordinates η and ζ, Eq. (A.3) is

$$T = A + B\, e^{\mu(\eta \cos\theta + \zeta \sin\theta)}. \tag{A.4}$$

This result is used in Section II and elsewhere.

Next, let us remove the restriction that no heat sources or sinks can be present but impose the additional condition that $\vec{e}_\eta$ and $\vec{e}_\xi$ are parallel (i.e., $\theta = 0$ and the ξ and η axes coincide). Thus, we shall consider one-dimensional steady-state heat conduction with heat addition or extraction and with motion of the solid in the direction of the temperature gradient. We shall assume that the energy per unit volume per second added to or extracted from the solid is given by $K(T_R - T)$, where K [energy/vol. sec. °K] is a positive constant and T_R is a constant reference temperature. Energy is added to the solid if $T < T_R$, while energy is extracted from the solid if $T > T_R$. The one-dimensional, steady-state heat equation now becomes

$$c\,\rho\, v\, dT/dx - \lambda d^2 T/dx^2 = K(T_R - T), \tag{A.5}$$

where x is the coordinate in the $\vec{v}$ direction. In terms of the reciprocal of the characteristic length,

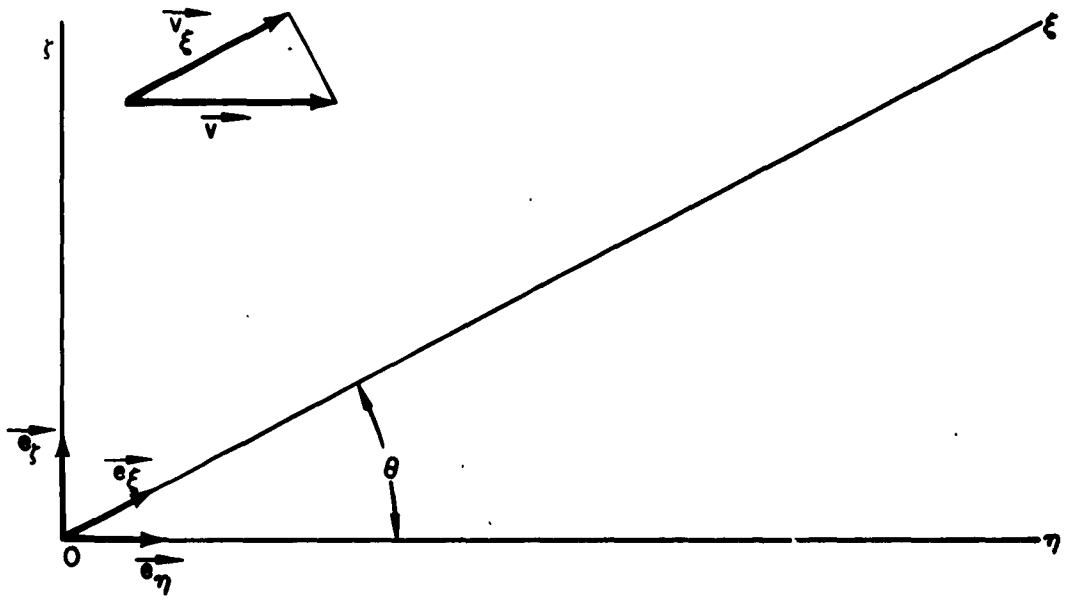

Figure A.1 THE ADOPTED CARTESIAN COORDINATE SYSTEM

$$\mu' \equiv \rho v c/\lambda$$

and the dimensionless heat transfer parameter,

$$\kappa' \equiv (4K/\lambda)/\mu'^2 ,$$

Eq. (A.5) can be written in the form

$$\mu' d(T - T_R)/dx - d^2(T - T_R)/dx^2 + (\mu'^2 \kappa'/4)(T - T_R) = 0. \quad (A.6)$$

The general solution to Eq. (A.6) is

$$T = T_R + a\, e^{\left[1 + \sqrt{1 + \kappa'}\right]\mu' x/2} + b\, e^{\left[1 - \sqrt{1 + \kappa'}\right]\mu' x/2} , \quad (A.7)$$

where a and b are arbitrary constants. Equation (A.7) is used in Sections IV and V.

REFERENCES

1. J. H. Grover, K. E. Rumble, M. L. Rice, L. L. Weil, A. W. Sloan and A. C. Scurlock, "Research and Development Programs in Fields of Solid Propellants and Interior Ballistics," Supplement to Quarterly Progress Report No. 26, Atlantic Research Corp., Alexandria, Va., July - September 1956.

2. M. Jacob, Heat Transfer, Vol. I, p. 558, John Wiley and Sons, New York (1949).